# Warm Events in the Tropical Atlantic

JAMES A. CARTON AND BOHUA HUANG

*Center for Ocean-Land-Atmospheric Interactions, Department of Meteorology, University of Maryland, College Park, Maryland*

## ABSTRACT

Sea surface temperature in the eastern equatorial Atlantic Ocean undergoes anomalous warming events of $1°-2°C$ every few years. The warm anomalies reach their maximum strength in Northern Hemisphere summer, when equatorial upwelling normally brings cold thermocline water to the surface. By compositing surface observations from a 28-year record, we are able to identify consistent features in anomalies of SST and winds. The composites show that the SST anomalies in northern summer are confined to the eastern equatorial region, with reduced zonal winds to the west and reduced northward trade winds to the east. Accompanying these changes in winds are enhanced convection near the equator caused by a southward shift and intensification of the intertropical convergence zone. Later in the year, SST south of the equator becomes elevated. As a result, by spring of the year following the equatorial anomaly, convection in the western side of the basin is much higher than normal.

To understand the ocean dynamics that give rise to these warm anomalies we examine a simulation of the ocean circulation during the 1980s. The authors find that the cause of the warm event in 1984 stretches back to the intense trade winds during the summer and fall of 1983. The unusual winds led to Ekman deepening of the thermocline in the west on both sides of the equator. Late in 1983 the trade winds in the west relaxed, which led to a surge of warm water eastward along the equatorial waveguide. The arrival of anomalous warm water deepened the thermocline throughout the eastern Gulf of Guinea in early 1984 and gradually spread southward and back into the interior basin throughout that year. Secondary factors in elevating equatorial SST were the local advection of warm surface water from the north and a reduction of advection of cool coastal water from the east. In contrast with 1984, the anomalous warming of 1988 seems to have been largely the result of changes in the equatorial winds during spring of the same year. These wind anomalies are likely, themselves, to have resulted from the increase in SST to the east. During both years anomalous deepening of the thermocline in the east (however it was caused) prevented the normal seasonal cooling of the equatorial waters and thus led to elevated SSTs. The eastward shift of heat also had important consequences for the coastal regions of southern Africa.

## 1. Introduction

The eastern equatorial Atlantic, like the eastern equatorial Pacific, undergoes strong seasonal changes in sea surface temperature (SST) in response to surface winds and heating. The major seasonal change in both oceans is the appearance in northern fall of cool thermocline water at the surface along the equator. Superimposed on this annual variation in the equatorial Pacific are the strong warm events of El Niño. During El Niño the anomalous oceanic changes prevent the seasonal appearance of cold SST. In this paper we discuss corresponding warm events in the tropical Atlantic. In the Atlantic, like the Pacific, these oceanic changes are closely linked to changes in the surface winds and heating. Thus we begin by looking for consistent features in the wind field during years with anomalous SST. We then explore how differing wind anomalies

can lead to elevated anomalies of SST by using numerical simulations of the ocean circulation to examine the warm events of 1984 and 1988.

In comparison with the Pacific, interannual fluctuations of variables such as SST in the Atlantic are weaker and have a broader range of scales as has been shown by Ward and Folland (1991) and Servain (1991). At decadal time scales tropical Atlantic SSTs undergo fluctuations that have patterns extending into midlatitudes with low amplitude near the equator. Anomaly patterns of this type have received attention from meteorologists because they are linked to rainfall changes over North Africa (Hastenrath and Lamb 1977; Lough 1986; Folland et al. 1986). However, at less than decadal time scales the SST anomalies are more closely confined to the eastern equatorial region. This latter pattern of fluctuation seems most similar to the warmings in the eastern Pacific, as suggested by Zebiak (1993), so we begin by examining the time history of eastern Atlantic SST fluctuations.

SST in the eastern equatorial Atlantic, like the eastern Pacific, is dominated by the seasonal cycle (Fig.

---

*Corresponding author address:* Dr. James A. Carton, Department of Meteorology, University of Maryland, College Park, MD 20742. e-mail: carton@cola.umd.edu
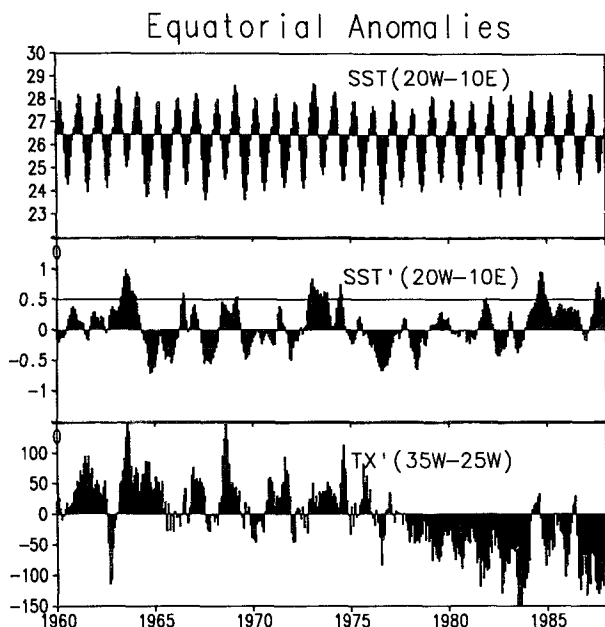
## Equatorial Anomalies



FIG. 1. Time series of (a) SST, (b) SST anomaly averaged 6°S–2°N, 20°W–10°E, and (c) zonal pseudostress anomaly 2°S–2°N, 35°W–25°W. Each time series has been smoothed with a 3-month running filter. SST (minus its mean value of 26.47°) and SST anomaly are expressed in °C, and stress in cm² s⁻². Warm years are those whose anomalies exceed 0.5°C for at least one month. Since 1960 this includes 1963, 1966, 1968, 1973, 1974, 1981, 1984, 1987, and 1988 (not shown).

1a). Temperatures reach their maximum in Northern Hemisphere spring, when the equatorial winds are weakest and the thermocline is deepest. During this season the sun is directly overhead, providing maximum incident solar radiation at the equator. However, the band of high SSTs (>27.5°C) extends well south of the equator to 8°S. As the year progresses the trade winds along the equator intensify as the southeast trade winds strengthen and the northeast trade winds weaken. The resulting zonal pressure gradient and associated uplifting thermocline leads to seasonal cooling of SSTs. The SSTs reach their minimum first along the eastern coast of Africa in July as a result of intensified coastal upwelling and then in the central Gulf of Guinea a month later.

Superimposed on these primarily annual variations of SST are anomalies that frequently exceed 0.5°C (Fig. 1b). During the 28-year period since 1960 nine such warm events have occurred. The first, in 1963, received attention partly because of its magnitude and partly because it coincided with the EQUALANT observational program (Katz et al. 1977; Merle 1980). The interval between successive warm events varies widely. The decade beginning in 1974 had few warm events relative to the surrounding decades of the 1960s and 1980s. As in the case of El Niño, the warm events in the Atlantic seem to be linked to the seasonal cycle, with the maximum

anomaly occurring in the equatorial upwelling zone in June and July (this is evident in the differing minimum temperatures from year to year in Fig. 1a).

The trade winds in the central basin also have strong, seasonal variations. The arrival along the equator of southeast trade winds in Northern Hemisphere spring intensifies both the westward and northward components of the equatorial winds. The anomaly from the seasonal trade wind (computed using a COADS analysis) shows variability on a variety of time scales (Fig. 1c). Throughout the 28-year period considered here the westward component has gradually intensified. Superimposed on this gradual intensification are shorter term fluctuations that bear a relationship to the fluctuations of SST. In most cases the onset of warmer SSTs is associated with a relaxation of the westward and northward components of the wind field (only the westward component is shown). In a statistical examination of this relationship for a 16-year period beginning in 1923, Servain et al. (1982) found that zonal wind anomalies explained 36% of the SST variance one month later. Here partly because of the presence of a long-term trend, the percentage of variance explained is less. Like SST anomalies, the wind anomalies are also locked to the seasonal cycle. Because of this phase locking, it seems appropriate to examine a composite of oceanic and atmospheric conditions during the years with warm events.

## 2. Composite analysis

Surface wind pseudostress $(\vec{U}|U|)$ and SST have been obtained from the COADS analysis of Woodruff et al. (1987) at 2° × 2° resolution for the period 1960–1987. The area we consider is limited to 10°S–20°N because of limitations in the data coverage. Convection is inferred from estimates of Outgoing Longwave Radiation provided by the NOAA Climate Analysis Center [its relationship to island rainfall is discussed in Yoo and Carton (1988)]. This data, corrected for orbit changes, is available at 2.5° × 2.5° resolution monthly for 1974–91 (except for a nine-month gap beginning March 1978). For each of these datasets monthly anomalies are computed with respect to the seasonal cycle computed from the full record. We shall composite years in which the SST anomaly in the eastern equatorial region (6°S–2°N, 20°W–10°E) exceeds 0.5°C for more than one month. This region, which is similar to the region defined by Zebiak (1993), is the region of largest near-equatorial SST variability. By this definition, eight warm events occurred prior to 1988: 1963, 1966, 1968, 1973, 1974, 1981, 1984, and 1987, while 1988 was itself unusually warm. For the composite analysis of convection, availability of the data restricts us to using the five years, 1974, 1981, 1984, 1987, and 1988.

For this presentation the monthly composites are averaged seasonally, using the conventional Northern

Hemisphere season definitions, spring (MAM), summer (JJA), fall (SON), and winter (DJF). Anomalies of vector winds are presented superimposed on anomalies of SST (Fig. 2a). Significance estimates for the individual anomalies of SST and the two components of wind stress are shown in Fig. 2b. Shaded areas indicate where the anomalies are not significant at the 95% confidence level (Bickel and Doksum 1977, 170–171).

Spring of the year in which the warm event occurs (year $Y$) is characterized by stronger than normal trade winds in the northeast and weak positive SST anomalies in the east, generally less than 0.25°C. By summer, when a tongue of cold surface water is normally present, a large area of abnormally warm water has formed along the equator between 15°W–5°E, extending well into the Southern Hemisphere. The westward component of the trade winds to the west of the warm anomaly is now weaker than normal. To the east the northward component is reduced as the result of a weaker than normal northwest African monsoon. By fall and winter the SST anomaly has broadened and shifted into the Southern Hemisphere, raising SSTs there by typically 0.5°C. This anomaly persists throughout spring of the following year.

Rainfall in the tropical Atlantic varies seasonally with the migration of the intertropical convergence zone (ITCZ), reaching its maximum latitude in fall. In spring it is at its minimum latitude, occasionally extending south of the equator (Fig. 3). The composite of OLR anomaly for the warm summers shows that the zonal band of rain associated with the ITCZ has expanded southward toward the warmer water. By spring of the following year (year $Y + 1$) anomalous rainfall has intensified, particularly in the northeastern coastal region of South America.

The appearance of enhanced convection over northern Brazil and reduced convection to the north, in fact, seems to result from the higher than normal SSTs in the Southern Hemisphere in the spring of year $Y + 1$. The extensive literature on the relationship between southern SSTs and Brazilian rainfall is reviewed in Hastenrath (1985). It is during this season that climatological conditions are most sensitive. Southern Hemisphere SSTs are highest, while the ITCZ is at its farthest southward displacement. Rainfall gauge data from the Nordeste region of Brazil show that the years with heaviest rainfall since 1960: 1964, 1967, 1974, and 1985, are all years following the years with anomalously warm equatorial SSTs (Ward and Folland 1991). Of these high rainfall years, the highest was 1985 when rainfall exceeded the normal by two standard deviations.

## 3. Model results

Some guidance for interpretation of the interannual changes described above can be obtained by examining the response of a numerical model of the tropical Atlantic Ocean to observed wind forcing. Here we use a primitive equation model originally developed by Philander and Pacanowski (1986), based on the GFDL model physics. The model is three-dimensional, including full advection equations for temperature and salt, with $1° \times \frac{1}{3}° \times 10$ m near-surface resolution in the tropics, expanding somewhat toward higher latitudes. The model has 27 levels in the vertical, for a total of 300 000 model grid points. A no-slip condition is imposed at the coasts as well as at the artificial north and south boundaries at 30°S and 50°N. To minimize the effects of the artificial boundaries, temperature and salinity at higher latitudes are relaxed to their monthly climatological values, thus minimizing coastal waves at high latitudes. Horizontal mixing and diffusion is parameterized by a constant coefficient of $2 \times 10^7$ cm$^2$ s$^{-1}$. The coefficients of vertical mixing and diffusion are Richardson number dependent, following Pacanowski and Philander (1981).

In this study our focus is on the response to anomalous winds. For this reason we use a climatological surface heating formulation. Net shortwave radiation is assumed to have a constant value corresponding to its climatological average between 10°S and 10°N, then to decrease linearly toward northern and southern boundaries. Longwave radiation is assumed to be a constant over the whole basin. Sensible and latent heating are estimated from a bulk formula that depends on the sea–air temperature difference calculated from climatological monthly air temperature and model derived SST at each grid point. For the main simulation the model has been integrated for nine years beginning January 1980, with initial conditions provided by a six-year integration using climatological seasonal wind stress. Monthly wind stress is computed from twice-daily 1000-mb wind analyses from the European Centre for Medium-Range Weather Forecasts (the availability of high-frequency winds was one reason for using the ECMWF winds rather than the COADS winds to drive the ocean model). Changes to the ECMWF wind analysis procedure that may introduce spurious low-frequency changes in the winds are described in Trenberth and Olson (1988). A full description of this simulation is provided in Huang (1992). Here we focus on changes, particularly of heat content, occurring in the ocean leading up to the warmings of 1984 and 1988, both in the model simulation, and also as they appear in the available observations. Observed and modeled summer SST anomalies for these two events are shown in Fig. 4. The SST anomaly in 1984 is first evident in the observations in spring at 10°S. Through the summer it spreads northward and strengthens. By fall and winter much of the equatorial Atlantic is above normal. In contrast, in 1988 the observed SST anomaly did not begin to develop until late spring. By the winter of 1988/89 tropical SST was below normal.
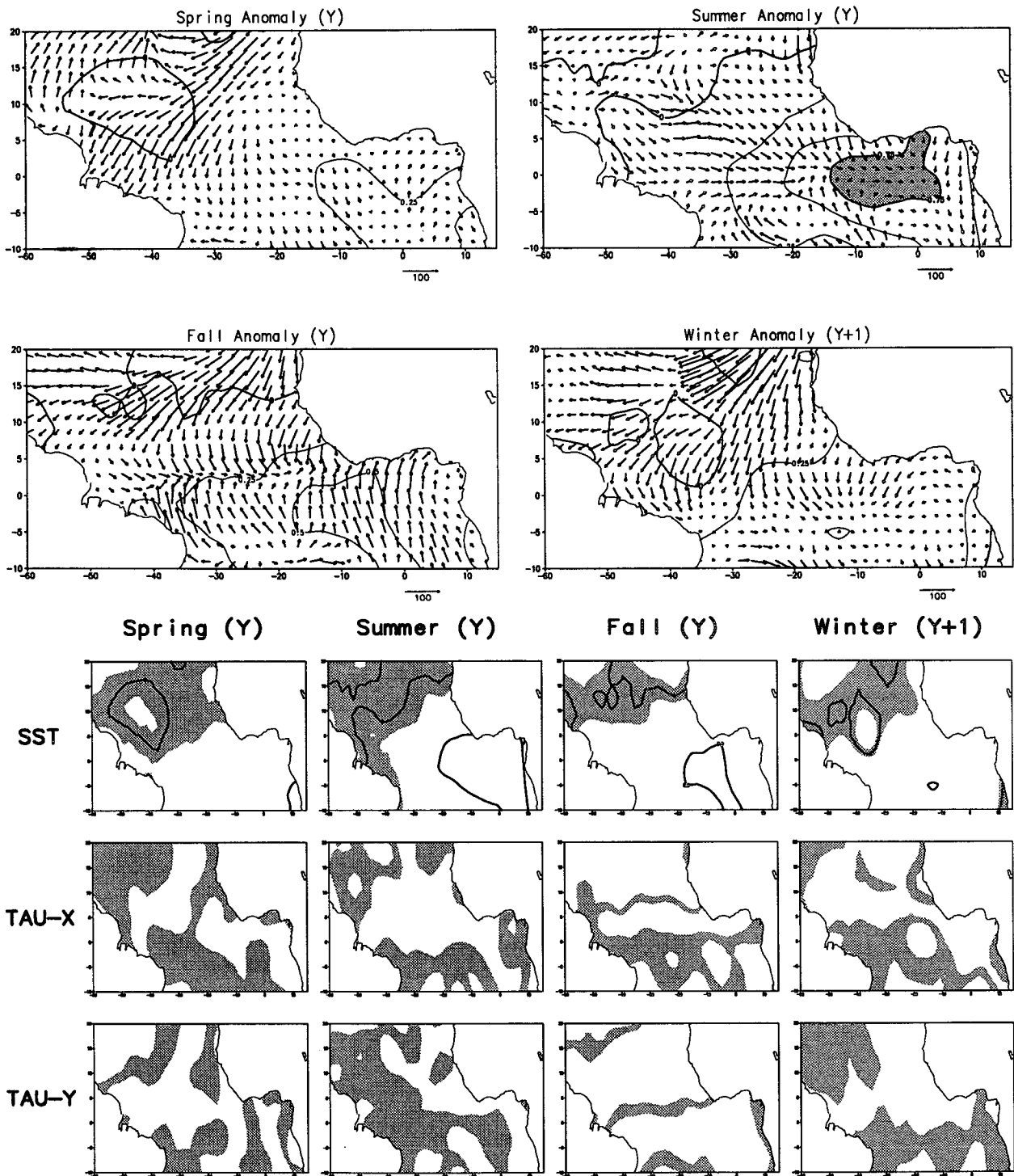
FIG. 2. (a) Composite of anomalous SST (contours) and wind pseudostress (vectors) for eight years with anomalously warm equatorial SST (see Fig. 1). Seasons shown are spring (MAM), summer (JJA), fall (SON) of the warm year, and winter (DJF) extending into the following year. SST contour interval is 0.25°C, while stress scale is given in cm$^2$ s$^{-2}$. Regions where the SST anomaly exceeds 0.75°C are shaded. The maximum anomalous SST occurs in the Gulf of Guinea in the Northern Hemisphere during summer. During this season the equatorial trade winds are anomalously weak in the west and the African monsoon is anomalously weak in the east. By the following winter the Southern Hemisphere is broadly warmer, while the northeast trades are intensified. (b) Significance estimates for the composite anomalies. Shaded areas indicate where the significance test fails at the 95% level.
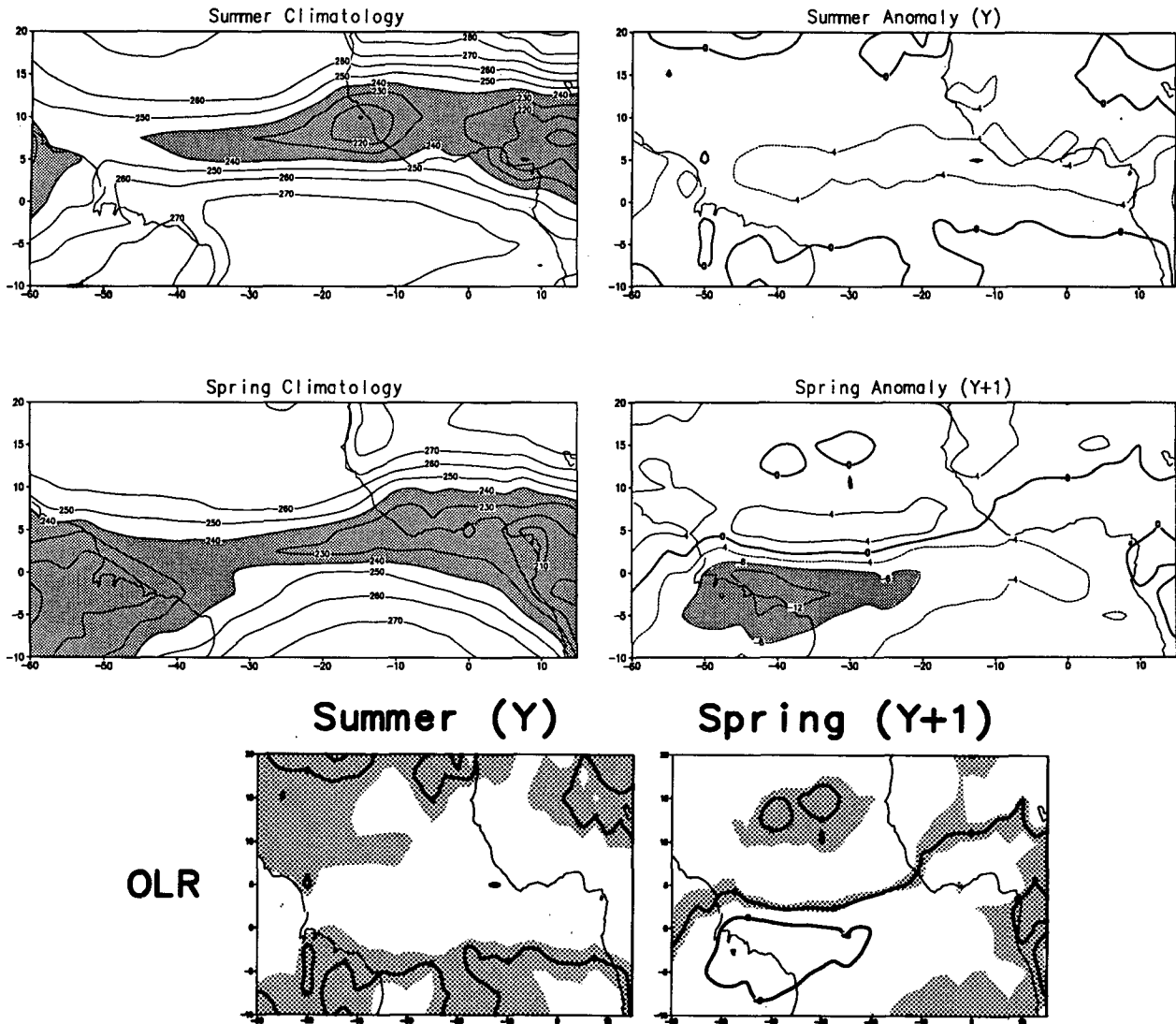
FIG. 3. (a) Summer and spring outgoing longwave radiation. Left-hand panels show climatological OLR computed from an 18-year dataset. Righthand panels show composite OLR anomalies for the summers of the years with warm events, and the spring of the following year. Composite is formed from the five warm events (1974, 1981, 1984, 1987, and 1988) that occurred since our record begins. Contour interval for climatology is 10 W m$^{-2}$, and the highly convective regions where OLR is below 240 W m$^{-2}$ are shaded. The contour interval for the anomalies is 2 W m$^{-2}$, and negative anomalies exceeding 6 W m$^{-2}$ are shaded. (b) Significance estimates for the composite anomalies. Shaded areas indicate where the significance test fails at the 95% level.

### a. 1984

By good fortune the SEQUAL/FOCAL experiment was conducted during 1982–84, and so the oceanographic data coverage is relatively extensive in the months prior to the 1984 warm event. It is evident from these observations that the origin of the 1984 event extends back into 1983. Early in 1983 the northern extension of the southeast trade winds in the western basin (which had been somewhat weak during the preceding year) intensified by 0.3 dyn cm$^{-2}$ (Fig. 5) as a result of changes in the winds and convection in the eastern Pacific. The trade wind anomaly during this period was primarily confined to a 10° band surrounding the equator; its narrow confinement led to anomalous heat storage in the west, both on and off the equator. On the equator, the thermocline deepened as a result of the intensified zonal trade winds. Off the equator, Ekman pumping caused downwelling rates of ⅓ m per day. In the west the unusual character of the trade winds was recorded at St. Peter and Paul's Rocks (2°N, 29°W), where the onset of the seasonal trades occurred a month early in 1983 and remained anomalously intense through the summer and fall. Late in 1983 the winds relaxed to near-normal conditions, while in the spring of 1984 the reappearance of the
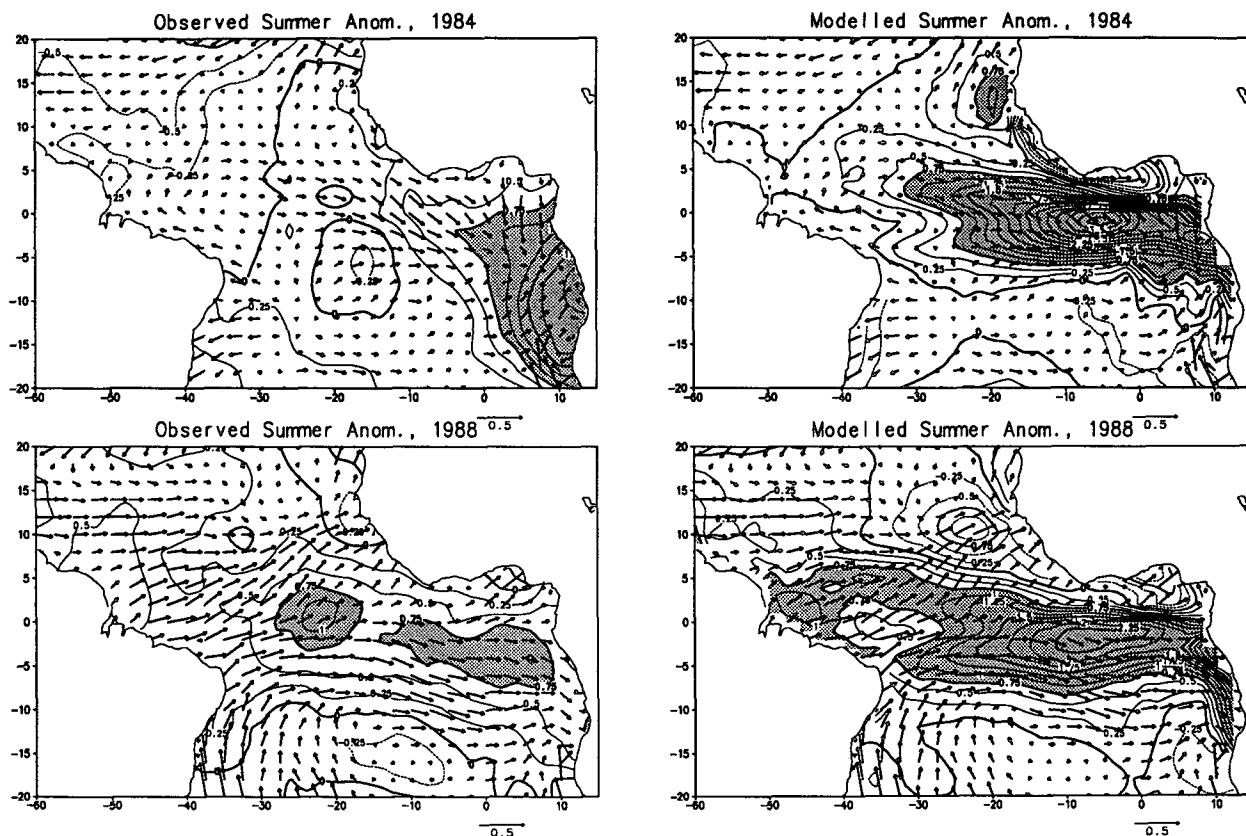
FIG. 4. SST and wind stress anomalies for summer 1984 and 1988. Left-hand panels show observed anomalies [ from the Reynolds ( 1988 ) analysis], while right-hand panels show SST anomalies produced by the simulation. SST anomalies greater than 0.75°C are shaded. Winds are given in dyn cm$^{-2}$.

trade winds occurred in May, as expected climatologically (Colin and Garzoli 1987). Rainfall was enhanced south of the equator in early 1984, indicating that the ITCZ had shifted anomalously southward, actually crossing the equator early in that year.

In the western basin the most continuous set of observations of subsurface temperature is provided by expendable bathythermograph records from a ship of opportunity transect between Brazil and Europe (Reverdin et al. 1991b). The depth of the 20°C isotherm along this transect (crossing the equator at approximately 30°W) is a useful estimate of the depth of the thermocline and also of the upper-ocean heat content. Throughout 1983 the observed thermocline along this transect was depressed by 5–10 m between 5°S and 5°N (Fig. 6). In January 1984 the thermocline in the west abruptly rose, so that through much of 1984 and 1985 the thermocline was 5–10 m shallower than normal. At 0°N, 30°W a 10-m shift of the thermocline approximately corresponds to a loss of 0.6°C averaged over 300 m, or 4.8 × 10$^4$ J cm$^{-2}$. This massive change in heat storage in the west in early 1984 coincided with a well-documented deepening of the thermocline (Katz 1987; Henin and Hisard 1987) and rising of sea level

(Cartwright et al. 1987; Verstraete 1992) in the eastern basin.

In the west the simulation, likewise, shows a large depression of the thermocline throughout 1983 and an abrupt rise by early 1984 (Fig. 7a,b,c); heat anomalies exceeding 6 × 10$^4$ J cm$^{-2}$ are shaded. Early in the year this buildup was most intense near the equator, while by July the largest anomalies were displaced poleward 7° to 10°. This large heat anomaly, corresponding to a 15 m depression of the thermocline, was maintained
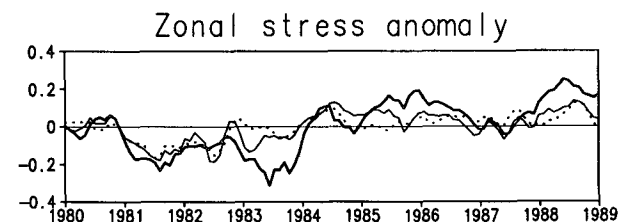


FIG. 5. Anomalous zonal wind stress in the equatorial Atlantic Ocean, 2°S, 2°N, averaged into three bands: (a) west (40°–25°W, bold), (b) central (25°–10°W, thin), and (c) east (10°W–5°E, dotted). Units are dyn cm$^{-2}$.
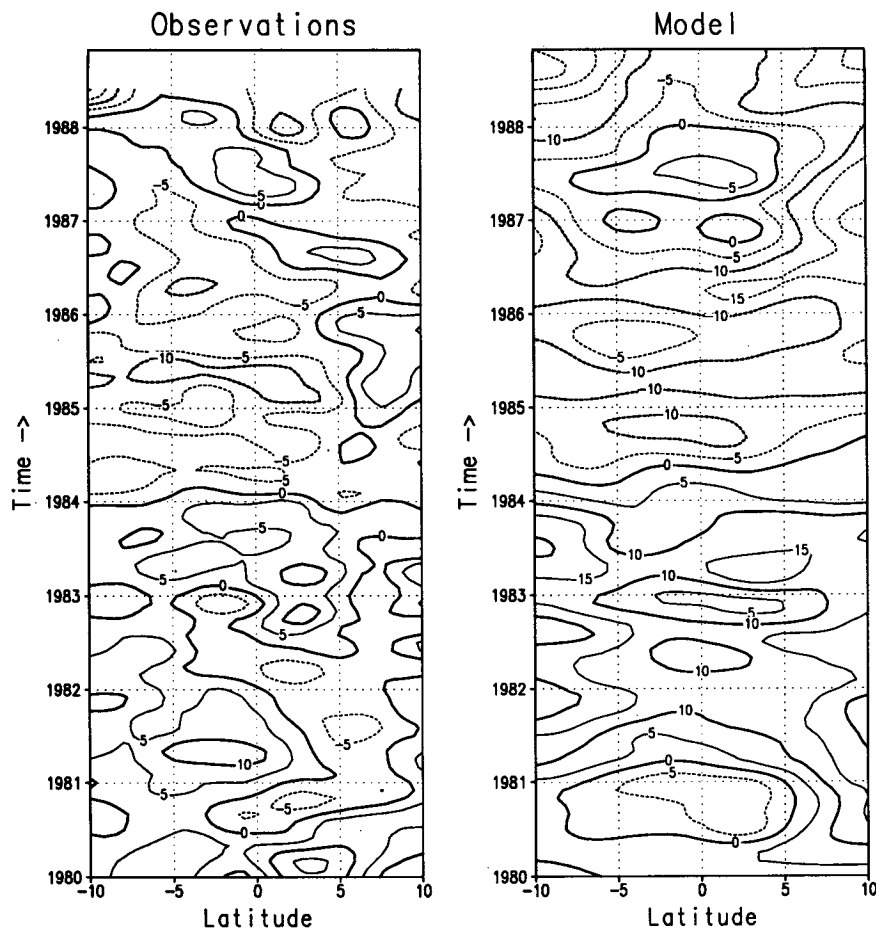
FIG. 6. 20°C-isotherm depth anomaly in the western tropical Atlantic during 1980–1988 [from objective analysis of ship of opportunity XBTs reported in Reverdin (1991b)]. Anomalies are computed with respect to the 9-year seasonal cycle. Depth anomalies are given in meters, positive downward. The transect runs southwest to northeast, crossing the equator at 30°W. Note the 10-m reduction in depth of the 20°C isotherm in early 1984 and less so in late 1987. The uncertainty associated with observed anomalies spanning many degrees of latitude may be less than 2 m (2% of the mean depth).

throughout the fall by the anomalously strong trade winds.

The relative importance of the two hemispheres in storing heat in the western basin is strongly affected by the geometry of South America and the consequent reduction of the dimension of the western Atlantic Ocean south of the equator, where the wind anomalies are largest (Fig. 5). It is also a function of the wind analysis used. It is interesting to compare these results with those we obtained when we repeated the simulation using the Servain and Legler (1986) winds. With the Servain and Legler winds, the buildup of heat in the Northern Hemisphere proceeded similarly to that shown in Fig. 7, while south of the equator the simulation had a much weaker heat anomaly and led eventually to a weaker SST anomaly in the summer of 1984.

The reduction of wind speeds of early 1984 no longer maintained excess heat storage in the west. Yet the amount of excess heat stored there was too great to be lost through surface fluxes (this would require an increase of heat flux of nearly 400 $Wm^{-2}$ to account for the rate at which heat was observed to leave). The real fate of this excess heat is apparent when we examine the changes that occur along the equator in the simulation (Fig. 8). Along the equator the trade winds weaken twice, first briefly in late July between 30° and 20°W and then again in August and September, and then weaken for an extended period beginning in November.

As a result of the weakening in July a pulse of heat anomaly is generated that crosses the basin in somewhat over a month. This pulse arrives in the Gulf of Guinea in mid-September and lasts until October, giving the pulse a total duration of one month and a speed of 60 cm s$^{-1}$. In linear equatorial ocean dynamics the most efficient way to move heat eastward along the
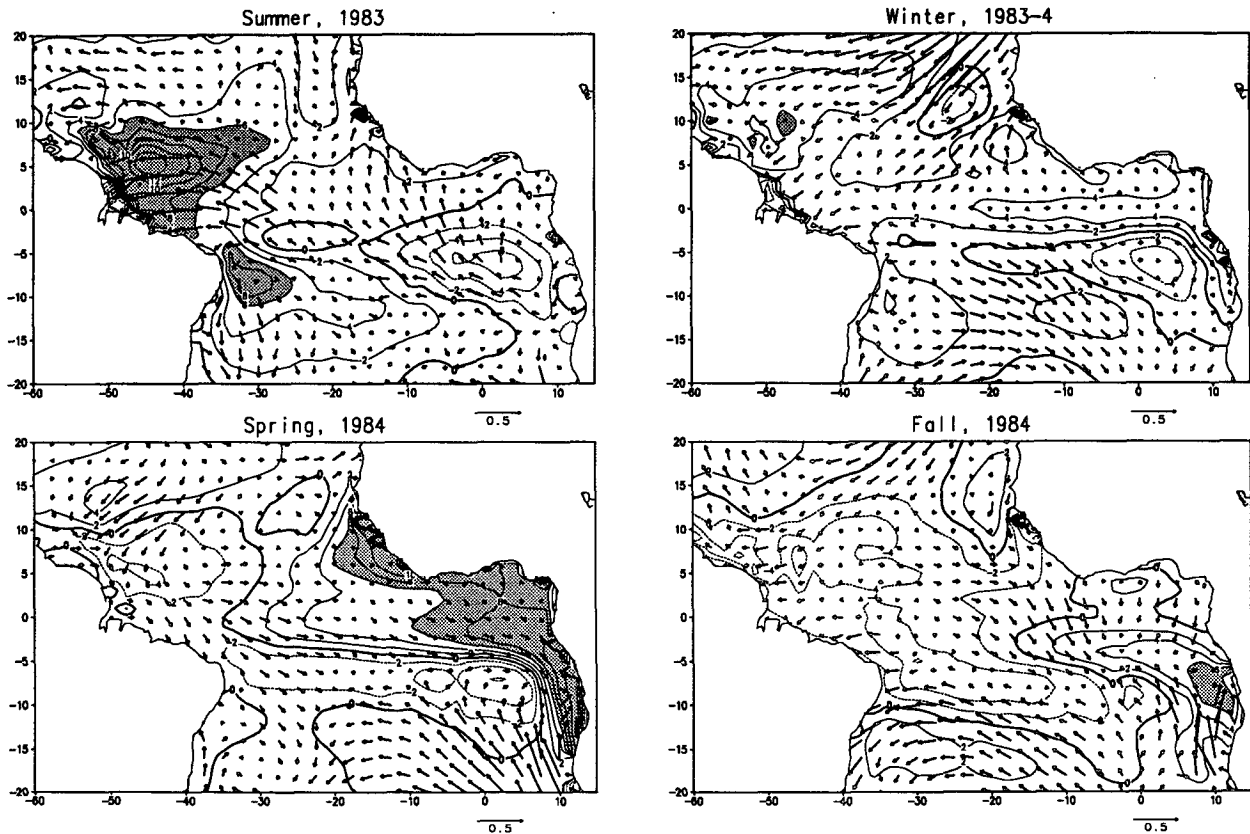
FIG. 7. Anomalous vector wind stress and heat content for 1983–84: (a) summer 1983, (b) winter 1983/84, (c) spring 1984, and (d) fall 1994. Stress is given in dynes cm$^{-2}$, while the contour interval of heat content is $2 \times 10^4$ J cm$^{-2}$. Shaded regions exceed $6 \times 10^4$ J cm$^{-2}$. Note the shift of heat from west to east with time following the relaxation of the trade winds in the west.

equator is in the form of an equatorial Kelvin wave (see, e.g., McCreary 1976). However, the eastward speed of the July pulse is a factor of 4 slower than expected for a freely propagating first baroclinic Kelvin wave. Examination of the vertical structure of the pulse shows that it has shorter vertical scales than expected for a first baroclinic wave (the spatial and temporal variations in stratification make an exact identification of vertical mode difficult).

However, the major transfer of heat from the western to eastern basin does not begin to occur in the simulation until November–December, when the winds west of 20°W reduce their strength by a third and are maintained in this reduced state throughout 1984 (Figs. 5 and 8). In response to this relaxation, a rapid surge of heat moves toward the east, leveling the depth of the thermocline along the equator within the month of December 1983. In the Gulf of Guinea the heat anomaly beginning in January exceeds 60 000 J cm$^{-2}$, with a constant transport of anomalous heat into the Gulf throughout the first few months of 1984. This anomalous eastward heat transport exceeds $2 \times 10^6$ J cm$^{-1}$ s$^{-1}$ and results from a weaker than normal westward current along the equator, as well as the deepening thermocline.

The first appearance of the simulated warm anomaly in early 1984 is accompanied by a weakening of the equatorial trade winds most strongly to the west of the region of warmer than normal SST. This relaxation seems to result from enhanced convergence over the warm water to the east. The relaxation has three effects on the ocean: 1) it reduces local upwelling of cold water, 2) it reduces westward advection of cold water, and 3) it reduces the zonal pressure gradient. The first two effects are local, while the third has its greatest importance to the east of the wind anomaly by deepening the thermocline.

By February 1984, the simulated thermocline in the east is at its maximum depth, more than 15 m deeper than normal in the zone of maximum temperature anomaly (4°S–2°N, 15°W–5°E). The deepened thermocline means that upwelling cannot effectively cool the surface. As a result, the SST becomes gradually warmer than its climatological value. This effect is particularly pronounced in the summer when the thermocline is shallowest and SST is at its climatological minimum. Thus while the maximum anomaly of heat appeared in the Gulf of Guinea in February 1984, the maximum anomaly of SST does not appear until mid-summer (Fig. 4). A similar delay between the maxi-
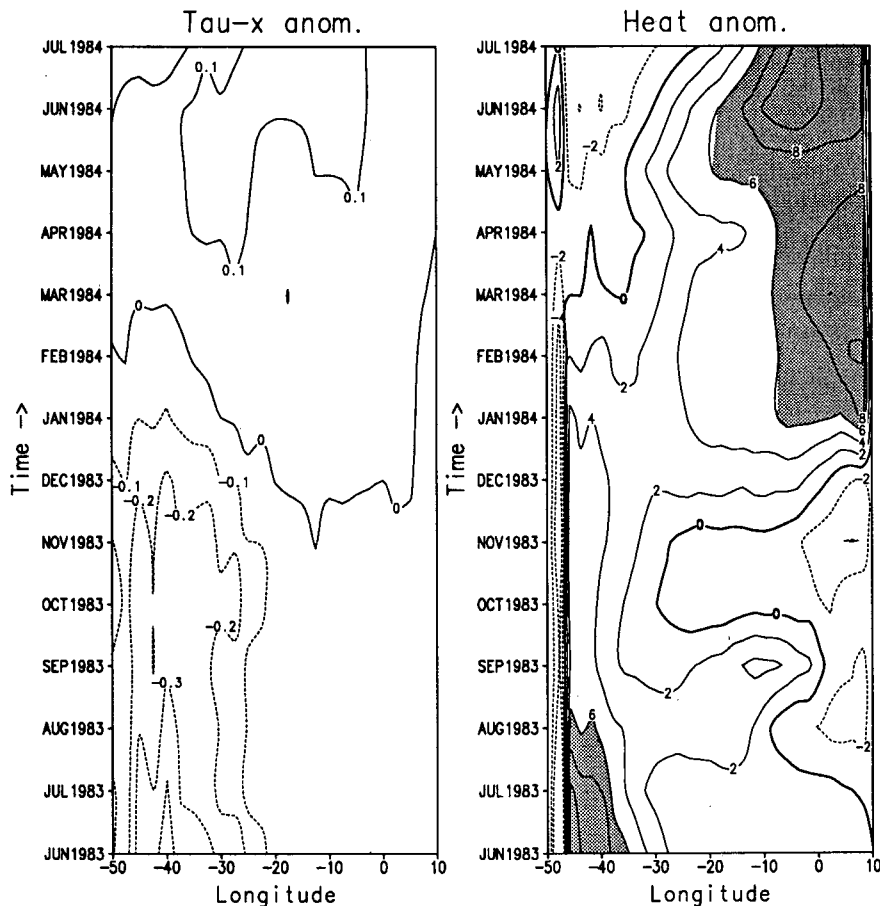
FIG. 8. Longitude-time sections along the equator of (left) anomalous zonal wind stress, and (right) anomalous upper-ocean heat content, for the period June 1983 to July 1984. The contour interval for wind stress is 0.1 dyn cm$^{-2}$, and for heat content is $2 \times 10^4$ J cm$^{-2}$. Heat anomalies exceeding $6 \times 10^4$ J cm$^{-2}$ are shaded.

mum displacement of the thermocline and the appearance of maximum SST anomaly was observed at 4°W (Houghton and Colin 1986).

Three experiments were carried out to examine the importance of preconditioning the ocean during 1983 on the development of the warm event in 1984. The first and second experiments examine the contribution of the oceanic state prior to June 1983 to the formation of the warm anomaly the following year. In the first experiment the simulation was restarted from the model's June climatology but was forced by observed winds beginning June 1983. Even though this experiment begins with no anomalous heat storage, by spring 1984 the heat anomaly in the Gulf of Guinea is three-fourths of the heat anomaly in the simulation (cf. Fig. 7c and Fig. 9a). Thus only one-quarter of the heat anomaly observed in the gulf in the spring resulted from winds before the second half of 1984. In the second experiment the simulation was again restarted on 15 June 1983, here using the 15 June 1983 simulation of the ocean state as initial conditions, but now relaxing

the winds to their seasonal climatology. In this experiment the ocean undergoes an abrupt transition in the summer of 1983, exporting heat to the Gulf of Guinea early and weakly. By the spring of 1984 there is only a weak temperature anomaly in the Gulf (Fig. 9b). In the third experiment the simulation was restarted six months later, on 15 January 1984, but like the first experiment, with initial conditions provided by the simulation climatology (Fig. 9c). Here as expected, the heat content anomaly in the following spring was weak and as a result only a mild SST anomaly developed.

The primary mechanism leading to anomalous SST during 1984 as well as 1988 in the eastern equatorial Atlantic is the reduction of heat flux out of the base of the mixed layer. In comparison with climatological conditions, the simulated thermocline in the region of the cold tongue remains anomalously deep throughout spring and summer in both years (Fig. 10a). This deepening reduces the rate at which cold subthermocline water is brought into the surface layer and thus
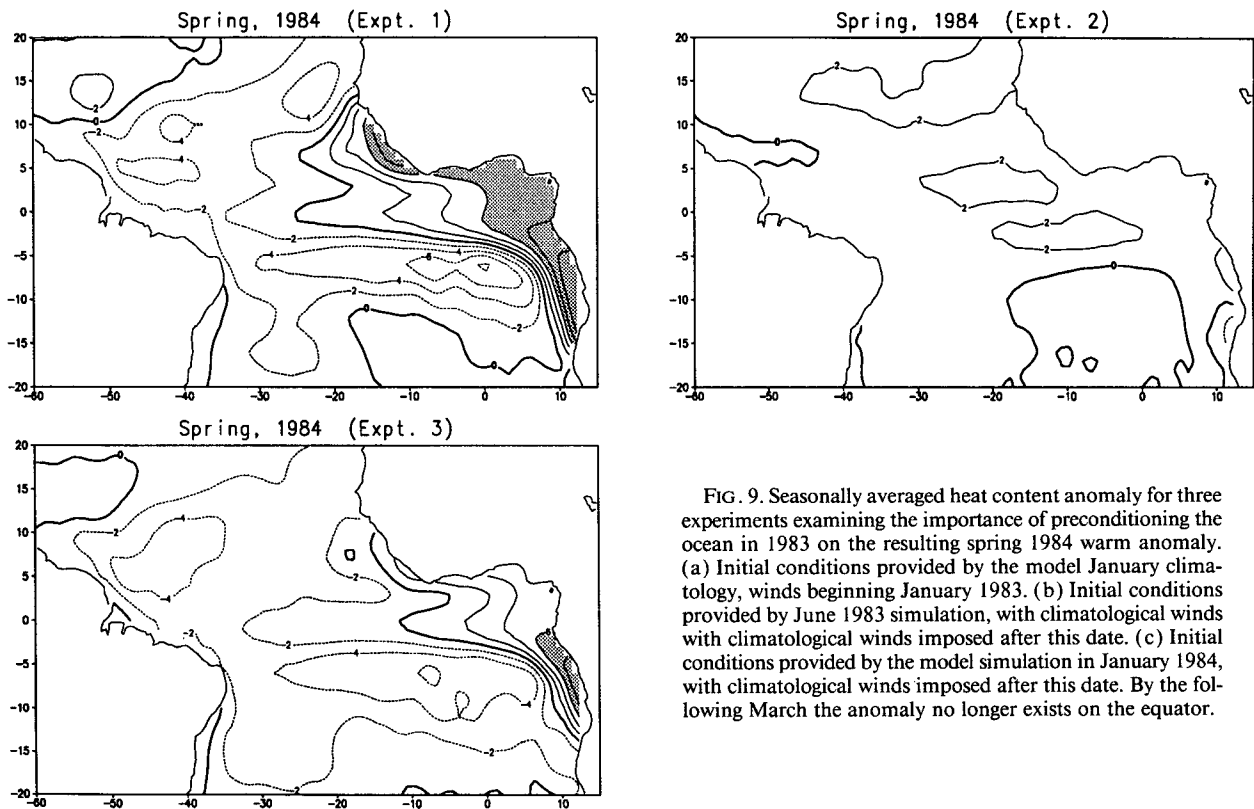
FIG. 9. Seasonally averaged heat content anomaly for three experiments examining the importance of preconditioning the ocean in 1983 on the resulting spring 1984 warm anomaly. (a) Initial conditions provided by the model January climatology, winds beginning January 1983. (b) Initial conditions provided by June 1983 simulation, with climatological winds with climatological winds imposed after this date. (c) Initial conditions provided by the model simulation in January 1984, with climatological winds imposed after this date. By the following March the anomaly no longer exists on the equator.

is responsible for the gradual increase of anomalous SST following the anomalous deepening of the thermocline in this region. Time series of anomalous SST and 20°C isotherm depth, shown in Fig. 10b, indicates that there is a negative correlation between these variables, with anomalous depressions of the thermocline preceding surface warming by a month or two. The spatial distribution of the correlation between these two variables is given in Fig. 10c. The correlation has its largest negative value in the region where anomalous SST variability is greatest, reaching a maximum magnitude of −0.75. However, in the southern central Atlantic and in some regions north of the equator, unusually warm SST is associated with a *shallow* 20°C isotherm depth. This relationship is mainly the result of multiyear time scale changes in oceanic variables, resulting from multiyear time scale changes in the wind field.

As indicated in Fig. 10c, there are large areas where changes in SST and thermocline depth are poorly correlated. In these regions zonal and meridional convergence of heat must also play an important role. In the summer of 1984 the simulated southward transport in the mixed layer north of the equator intensified (Fig. 10a). This anomalous transport carried warm near-coastal water into the equatorial zone. In addition to increasing meridional heat transport, this mass con-

vergence in the meridional direction, which was due to local changes in the wind field, had the effect of further depressing the thermocline. In contrast, in 1988 the equatorial winds had a northward anomaly, leading to northward surface currents at the equator.

Changes in zonal heat transport also occur. The simulated increase in SST progressing eastward from 5°W to the coast normally varies from 0°C in January to −3°C in August. In 1984 this gradient was reduced to between 0° and 2.5°C. At the same time, the westward current was reduced. Both of these anomalies have the effect of reducing the normal cooling effect of westward transport of upwelled coastal water into the equatorial zone.

Throughout the spring of 1984 the excess heat present in the Gulf of Guinea in the simulation surges poleward symmetrically in the two hemispheres, northward along the coast of northwest Africa and southward along Angola, becoming more coastally trapped with latitude. Observations from sea-level records along the southern coast of Africa show elevated sea level as far south as Walvis Bay (23°S, where the anomaly exceeded 5 cm) and beyond (Brundrit et al. 1987). Surface water was observed to be carrying warm, high-salinity, tropical water anomalously southward, so that at 50 m, anomalies of 2°C and 0.2 psu were observed off central Namibia. This had the effect of
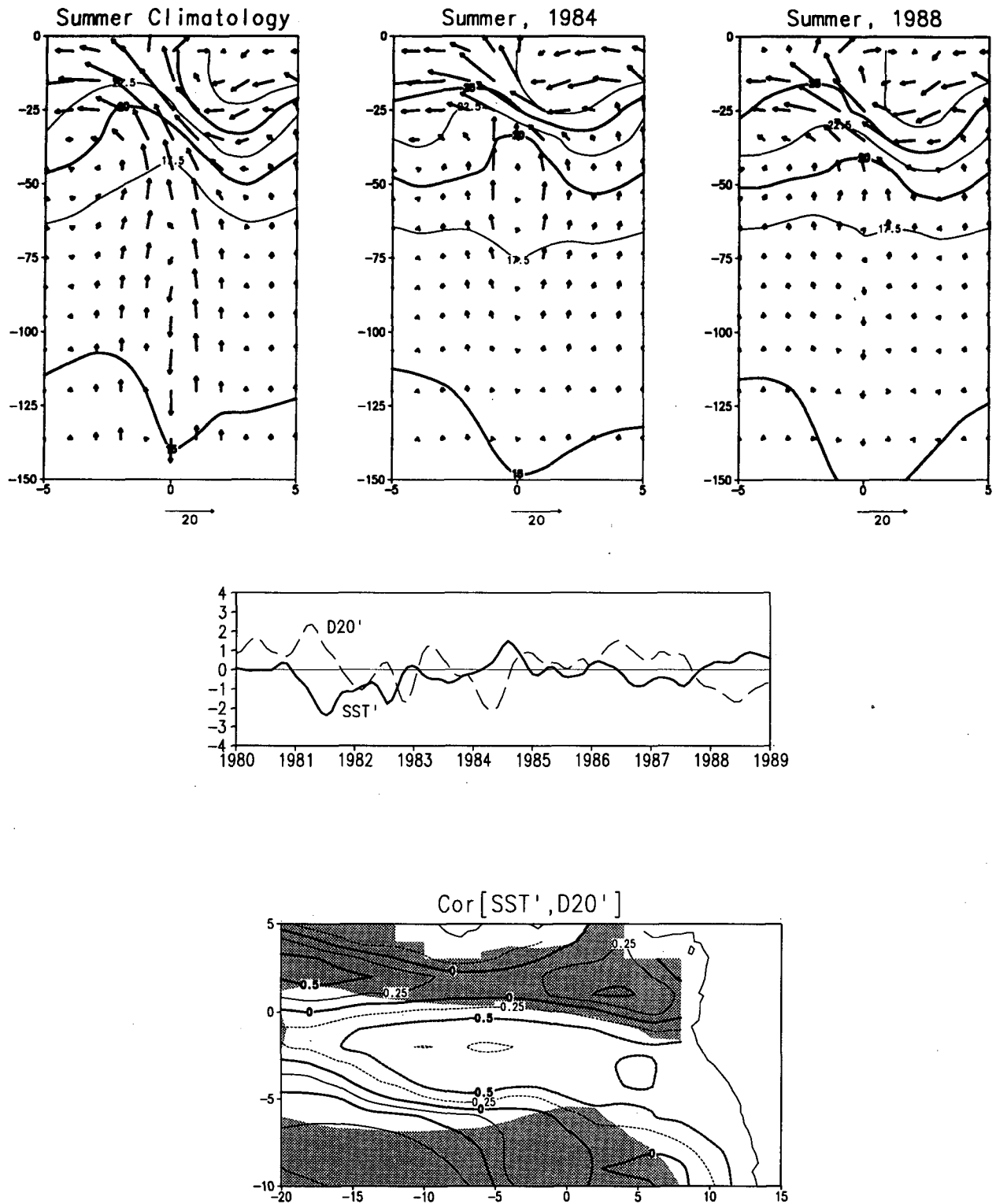
FIG. 10. Conditions in the eastern Atlantic, averaged 15°W–5°E. (a) Summer temperature and velocity $(v, w)$ with depth and latitude. Temperature contour interval is 2.5°C. Velocity is given in cm s$^{-1}$ $(v)$ and 10$^{-4}$ cm s$^{-1}$ $(w)$. (b) Anomalous SST (bold) and 20°C isotherm depth (thin dashed) variations in the eastern equatorial Atlantic (also averaged meridionally 6°S–2°N). SST is given in units of 1°C. Depth is given in units of 5 m. Periods of anomalously warm (cold) SSTs in 1984 and 1988 are preceded by anomalous deepening (shallowing) of the thermocline. (c) Correlation between anomalous SST and 20°C isotherm depth variations in the eastern tropical Atlantic. Regions where the variance of anomalous SST is less than 0.5(°C)$^2$ are shaded.

suppressing Benguela upwelling of cool water, despite stronger than normal upwelling-favorable winds (Shannon et al. 1986). An examination of the simulation in February 1984 shows the rapid southward extension of the warm tropical water with coastal temperature anomalies at 45 m depth in excess of 5°C and salinity anomalies exceeding 0.1 psu (Fig. 11). Anomalous currents of 20 cm s$^{-1}$ are the geostrophic result of these changes in heat distribution and cause an anomalous "south equatorial countercurrent" (SECC) in the Gulf of Guinea, which, however, is not dynamically similar to the north equatorial countercurrent (NECC). By fall the temperature anomalies near the coast were reduced to 3°C, with current anomalies less than 5 cm s$^{-1}$.

Since the incident heat anomaly is symmetric about the equator, the heat anomalies that move poleward in the two hemispheres are also initially of equal strength. However, after leaving the equator the heat anomaly moving eastward and then northward out of the gulf weakens, so that the largest remaining heat anomaly is south of the equator (Fig. 7d). An interesting dynamical question arises as to why the southern heat anomaly persists while the northern anomaly weakens. Possible causes of this include effects of the differences in the mean flow between the two hemispheres. Chang and Philander (1989) point out that the presence of the eastward NECC in the Northern Hemisphere reduces the westward component of group velocity for equatorial waves, causing the anomalies to remain trapped near the coast, while the westward flow of the SEC in the Southern Hemisphere enhances westward propagation. For this reason anomalies may be expected to extend much farther into the ocean in the Southern Hemisphere. Local processes such as surface cooling and Ekman pumping (strong off northwest Africa), and coastal geometry may also play important roles.

More so than the temperature field, changes in currents from year-to-year have been difficult to estimate based on observations and have led to some confusion about the mechanism by which excess heat was brought into the Gulf of Guinea in 1984. Henin and Hisard (1987) and Hisard and Henin (1987) suggested from direct instantaneous measurements and geostrophic calculations that the NECC was unusually well developed in 1984. This led Henin and Hisard to suggest that the NECC provided anomalous eastward transport of heat and thus was directly responsible for the 1984 warming. However, geostrophic calculations by Reverdin et al. (1991a) using VOS XBT records and Katz (1993) using Inverted Echo Sounder time series show that the transport by the NECC was actually significantly weaker than normal in 1984. The cause of these apparently contradictory observations is unclear. An alternative (Southern Ocean) explanation was put forward by Philander (1986), who proposed that "an unusual eastward current south of the equator" was re-
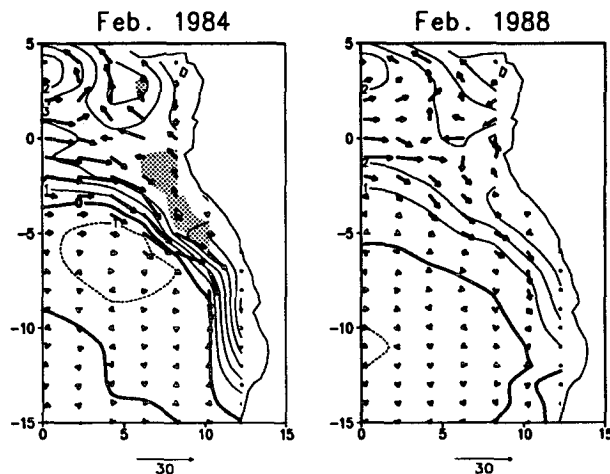


FIG. 11. Simulated anomalous temperature, salinity, and currents at 45-m depth in the southern Gulf of Guinea. (a) February 1984; (b) February 1988. Contour interval is 1°C. Velocities are given in cm s$^{-1}$. Regions where the anomalous salinity exceeds 0.1 psu are shaded.

sponsible for the anomalous eastward transport. Neither of these explanations is consistent with the results from this simulation. Here the simulated NECC volume and heat transports are lower than normal during 1984. The near-surface currents more than a few degrees south of the equator gradually slow down throughout the 1980s, as the southeast trade winds weaken, without any sudden changes in 1984. Only the anomalous tropical of heat eastward along the equator by equatorial waves can explain the deepening of the thermocline in the Gulf of Guinea in 1984.

### b. 1988

Throughout 1985–86 the equatorial winds were weaker than normal, returning to near-normal values during 1987, while the northeast trades were somewhat more intense than normal. South of the equator the winds continued to weaken throughout this period. Observed movements of the thermocline in the west reflected these changes in the wind field. During most of 1985–86 the thermocline was observed to be 5–10 m shallower than normal except north of 5°N (Fig. 6). This meridional anomaly of thermocline depth reduced the seasonal south-to-north pressure gradient. Consistent with this, Katz's (1992) examination of Inverted Echo Sounder records shows reduced NECC transport throughout 1984–86 at 38°W, with the minimum occurring in 1986. The simulated NECC transport is also reduced but not as strongly as observed. Along the equator in the east, SST was observed to reach its minimum in 1986, with the most negative anomaly of 1°C developing late in that year.

By spring of 1987 the northeast trade winds north of 5°N had weakened significantly. This weakening,

and the resulting Ekman convergence, led to a deepening of the thermocline in the west between the equator and 5°N throughout that season in both the observations and the simulation. The deepening of the thermocline near the equator also had an effect on the currents farther north by increasing the equatorward pressure gradient and thus strengthening the NECC (Katz 1992). In contrast with 1983, in 1987 only about half as much anomalous heat was observed in the western transect (Fig. 6). Analysis of Geosat altimeter observations for this period (Carton and Katz 1990) also suggest modestly higher sea level in late 1987 in the western Atlantic where elevated sea level is well correlated with a depressed thermocline.

Throughout summer and fall of 1987 the northeast trades strengthened to the north and then generally weakened throughout the basin by 30%. This relaxation preceded an eastward shift of anomalous heat (Fig. 12). If the wind had returned to climatological conditions in mid-1987, the 1988 warming would not have occurred. However, the warming of SSTs along the equator through the fall of 1987, and winter and spring of 1988, was accompanied by a dramatic weakening of the equatorial trade winds to the west. This weakening was similar to that of 1983 but was stronger and lasted much longer. As a result, the heat anomaly grew

continuously from October 1987 through January 1988, and then remained in the central basin for the remainder of the year (Fig. 12). In both 1984 and 1988 the largest anomalies of heat were located east of 20°W, while the strongest wind anomalies occurred to the west of this longitude (cf. Figs. 8 and 13).

By May 1988, a season in which the equatorial winds normally intensify, the trade winds in the western tropical region had nearly collapsed, with stresses less than 0.1 dynes cm$^{-2}$. The heat anomaly in the east had increased to levels similar to 1984, leaving negative heat anomalies in the west as a result of the weakened trade winds. In the east the thermocline remained depressed by 10 m through the first half of 1988. As in 1984, the depression of the thermocline reduced the vertical flux of heat out of the layer of active mixing, allowing SST to rise (Fig. 10). As in the case of 1984, the major part of the heat content anomaly moved southward in fall, with only a small fraction progressing northward (Fig. 12d).

## 4. Discussion

The eastern tropical Atlantic is characterized by events with anomalously warm SSTs. These events occur in varying strengths every few years. The timing of
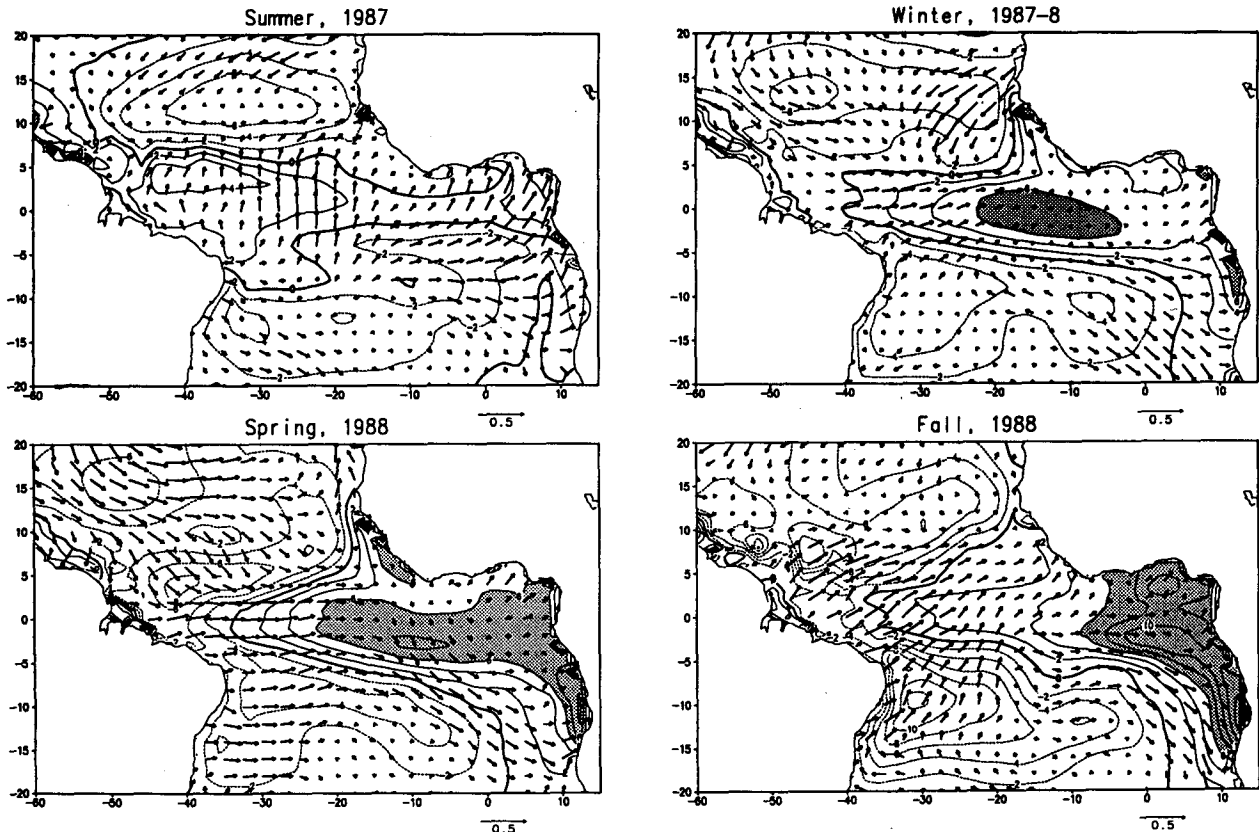


FIG. 12. The same as Fig. 6 except for the periods of (a) summer 1987, (b) winter 1987/88, and (c) spring 1988 and fall 1988.
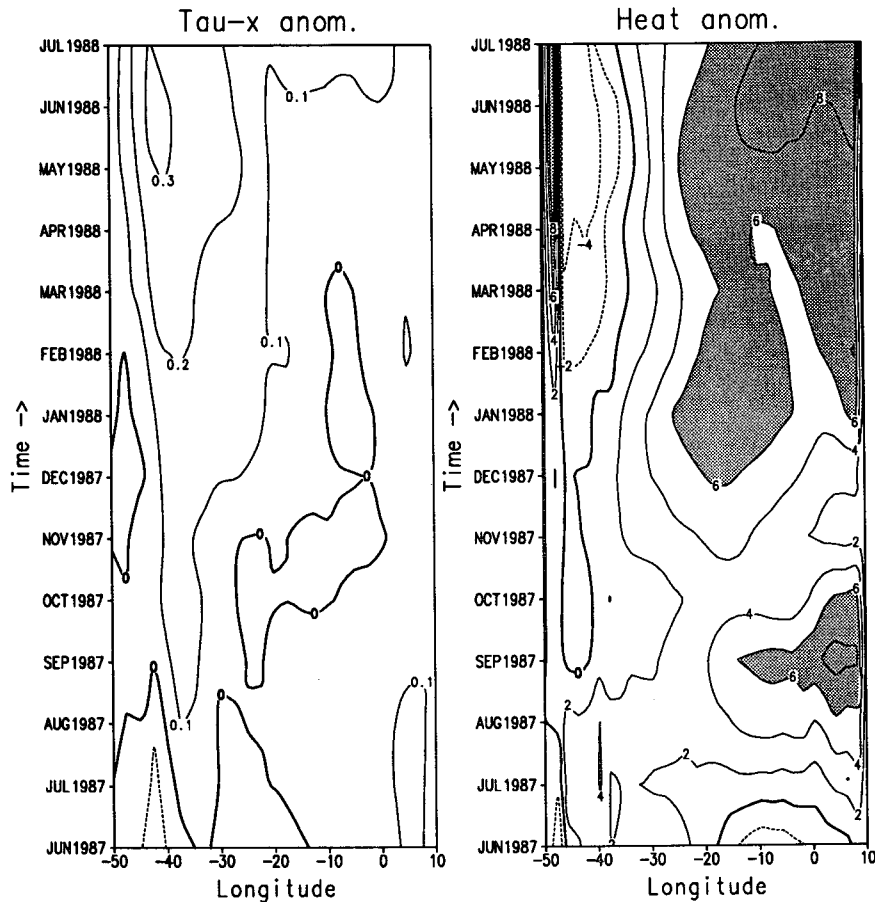
FIG. 13. Same as Fig. 8 except for the period of June 1987 to July 1988.

the warm events is linked to the seasonal cycle, so that the maximum anomaly occurs during the normally cold northern summer–fall. By winter a broad weak warm anomaly appears south of the equator and gradually spreads westward during the first half of the year following the warm event. The warm SST anomalies are accompanied by changes in the surface winds. These changes frequently include a weakening of the northeast trade winds early in the year and a relaxation of the southeast trade winds along the equator in the spring to the west of the region where the anomalously warm SST develop. The relaxation of the trade winds in midbasin has profound effects on the equatorial thermocline. In 1984 and 1988 the relaxation contributed to a deepening of the thermocline in the eastern basin by 10 m. This deepening reduced the vertical flux of heat out of the near-surface layer, leading to a strengthening of the SST anomaly. The similarities between these changes and the changes associated with El Niño in the Pacific are striking.

Yet an examination of convection in the atmosphere shows that there are significant differences between the Atlantic and Pacific. In contrast to the eastern Pacific,

the eastern equatorial Atlantic has strong seasonal convection. Anomalies of convection during warm events are primarily associated with a southward shift and intensification of the intertropical convergence zone, in contrast to the eastward shift with time observed in the Pacific. The likely reason for these differences is the extra geographic control over the position of convective zones in the Atlantic because of the presence of the African and South American continents. Other reasons may be the smaller amplitude and shorter duration of the fluctuations of SST in the Atlantic.

A second difference between events in the Atlantic and Pacific has to do with the relative influence of the global circulation. It is accepted that El Niño is the result of unstable interactions between the Pacific Ocean and its overlying atmosphere. It seems that the initial cause of many of the warm events in the Atlantic may be traced back to changes in the large-scale wind field that do not have their origin in the Atlantic. Our analysis of the origin of the 1984 event suggests the major cause of anomalous warming was the ocean's response to a change in the wind field in the western

basin. The 1984 event, unlike 1988, was preceded by a massive buildup of anomalous heat in the western Atlantic. The relaxation of the trade winds in the western basin in late 1983 was followed by a surge of this heat into the Gulf of Guinea. In this case the Atlantic Ocean is acting to some extent as a passive guide through which heat is shifted from west to east in response to changes in the wind field. A mechanism similar to this was originally suggested by Moore et al. (1978) to explain the seasonal cycle of tropical Atlantic SST. In 1988 the great increase in heat content occurred in midbasin in the spring. The cause of this increase was a relaxation of the equatorial trade winds just to the west of the heat anomaly. This relaxation reduced the seasonal upwelling and weakened the zonal pressure gradient, further amplifying the heat anomaly.

Like their Pacific counterpart, warm events in the tropical Atlantic have broad climate effects. We have shown that rainfall increases along the northern Gulf of Guinea during the normally dry summer months. On the western side of the basin, along the northeast coast of South America, seasonal rainfall normally occurs in spring. In the spring of the year after a warm event, this rainfall is enhanced, contributing to the floods that plague the Nordeste region of Brazil. The eastward shift of heat along the equatorial waveguide, which is mainly responsible for the elevated SSTs in the simulation, also causes a variety of changes along the southern coast of Africa. These include a reversal of the normally equatorward Benguela Current, and a southward intrusion of warm, saline tropical water. Observations confirm the appearance of these anomalous physical changes during years with warm events (Mazeika 1968; Shannon et al. 1986; Brundrit et al. 1987). The resulting effects on the fish and bird populations are profound (Crawford et al. 1990).

Several factors make interannual variability of the tropical Atlantic more complex than that of the tropical Pacific. Perhaps the most important is that the Atlantic appears to support a wider variety of phenomena, including modes of variability that are not confined to the tropics. The position of continents and the geometry of their coastlines add complexity. Yet the observational network in the equatorial Atlantic is currently very limited. The results presented here suggest that continued progress in understanding the dynamics of variability in the tropical Atlantic will require a much expanded observational network.

## REFERENCES

Bickel, P. J., and K. A. Doksum, 1977: *Mathematical statistics: Basic Ideas and Selected Topics.* Holden-Day, 492 pp.

Brundrit, De Cuevas, and A. M. Shipley, 1987: Long-term sea-level variability in the eastern south Atlantic and a comparison with that in the eastern Pacific. *The Benguela and Comparable Ecosystems,* A. I. Payne, J. A. Gulland, and K. H. Brink, Eds., S. *African J. Mar. Sci.,* 5, 73–78.

Carton, J. A., and E. J. Katz, 1990: Estimates of the zonal slope and seasonal transport of the Atlantic North Equatorial Countercurrent. *J. Geophys. Res.,* 95, 3091–3100.

Cartwright, D. E., R. Spencer, and J. M. Vassie, 1987: Pressure variations on the Atlantic equator. *J. Geophys. Res.,* 92, 725–741.

Chang, P., and S. G. H. Philander, 1989: Rossby wave packets in baroclinic mean currents. *Deep-Sea Res.,* 36, 17–37.

Colin, C., and S. L. Garzoli, 1987: In situ wind measurements and the ocean response in the equatorial Atlantic during the Programme Francais Ocean et Climat Dans l'Atlantic Equatorial and Seasonal Response of the Atlantic Ocean Experiment. *J. Geophys. Res.,* 92, 3741–3750.

Crawford, R. J. M., W. R. Siegfried, L. V. Shannon, C. A. Villacastin-Herroro, and L. G. Underhill, 1990: Environmental influences on marine biota off southern Africa. *S. African J. Sci.,* 86, 330–339.

Folland, C. K., T. N. Palmer, and D. E. Parker, 1986: Sahel rainfall and worldwide sea temperatures. *Nature,* 320, 602–606.

Hastenrath, S., 1985: *Climate and Circulation of the Tropics.* D. Reidel Publishing Co., 455 pp.

——, and P. J. Lamb, 1977: Some aspects of circulation and climate over the eastern equatorial Atlantic. *Mon. Wea. Rev.,* 106, 1280–1287.

Henin, C., and P. Hisard, 1987: The North Equatorial Countercurrent observed during the Programme Francais Ocean et Climat Dans l'Atlantic Equatorial Experiment in the Atlantic Ocean, July, 1982 to August, 1984. *J. Geophys. Res.,* 92, 3751–3758.

Hisard, P., and C. Henin, 1987: Response of the equatorial Atlantic Ocean to the 1983–4 wind from the FOCAL cruise data set. *J. Geophys. Res.,* 92, 3759–3768.

Houghton, R. W., and C. Colin, 1986: Thermal structure along 4°W in the Gulf of Guinea during 1983–4. *J. Geophys. Res.,* 91, 11 727–11 740.

Huang, B., 1992: Numerical simulation of the seasonal and interannual variability of the tropical Atlantic Ocean circulation during the 1980s. Ph.D. dissertation, University of Maryland, 209 pp.

Katz, E., and others, 1977: Zonal pressure gradient along the equatorial Atlantic. *J. Mar. Res.,* 35, 293–307.

——, 1987: Seasonal response of the sea surface to the wind in the equatorial Atlantic. *J. Geophys. Res.,* 92, 1885–1893.

——, 1993: An interannual study of the Atlantic North Equatorial Countercurrent. *J. Phys. Oceanogr.,* 23, 116–123.

Lough, J. M., 1986: Tropical Atlantic sea surface temperatures and rainfall variations in sub-Saharan Africa. *Mon. Wea. Rev.,* 114, 561–570.

Mazeika, P. A., 1968: Eastward flow within the South Equatorial Current in the eastern South Atlantic. *J. Geophys. Res.,* 73, 5819–5828.

McCreary, J., 1976: Eastern tropical ocean response to changing wind systems with application to El Niño. *J. Phys. Oceanogr.,* 6, 632–645.

Merle, J., 1980: Variabilite thermique et interannuelle de l'Ocean Atlantique equatorial Est. L'hypothese d'un "El Niño" Atlantique. *Oceanol. Acta,* 3, 209–220.

Moore, D. W., P. Hisard, J. P. McCreary, J. P. Merle, J. O'Brien, J. J. Picaut, J. M. Verstraete, and C. Wunsch, 1978: Equatorial adjustment in the eastern Atlantic. *Geophys. Res. Lett.*, **5**, 637–640.

Pacanowski, R. C., and S. G. H. Philander, 1981: Parameterization of vertical mixing in numerical models of tropical oceans. *J. Phys. Oceanogr.*, **11**, 1443–1451.

Philander, S. G. H., 1986: Unusual conditions in the tropical Atlantic Ocean in 1984. *Nature*, **322**, 236–238.

——, 1990: *El Niño, La Niña, and the Southern Oscillation.* Academic Press, 293 pp.

——, and R. C. Pacanowski, 1986: A model of the seasonal cycle of the tropical Atlantic Ocean. *J. Geophys. Res.*, **91**, 14 192–14 206.

Reverdin, G., P. Delecluse, C. Levy, P. Andrich, A. Moliere, and J. M. Verstraete, 1991a: The nearsurface tropical Atlantic in 1982–4: Results from a numerical simulation and a data analysis. *Prog. Oceanogr.*, **27**, 273–340.

——, P. Raul, Y. DuPenhoat, and Y. Gouriou, 1991b: Vertical structure of the seasonal cycle in the central equatorial Atlantic Ocean: XBT sections from 1980 to 1988. *J. Phys. Oceanogr.*, **21**, 277–291.

Reynolds, R. W., 1988: A real-time global sea surface temperature analysis. *J. Climate*, **1**, 75–86.

Servain, J., 1991: Simple climatic indices for the tropical Atlantic Ocean and some applications. *J. Geophys. Res.*, **96**, 15 137–15 146.

——, and D. M. Legler, 1986: Empirical orthogonal function analysis of tropical Atlantic sea surface temperature and wind stress: 1964–1979. *J. Geophys. Res.*, **91**, 14 181–14 191.

——, J. Picaut, and J. Merle, 1982: Evidence of remote forcing in the equatorial Atlantic. *J. Phys. Oceanogr.*, **12**, 457–463.

Shannon, L. V., A. J. Boyd, G. B. Brundrit, and J. Taunton-Clark, 1986: On the existence of an El Niño type phenomenon in the Benguela system. *J. Mar. Res.*, **44**, 495–520.

Trenberth, K. E., and J. G. Olson, 1988: An evaluation and intercomparison of global analyses from the National Meteorological Center and the European Centre for Medium-Range Weather Forecasts. *Bull. Amer. Meteor. Soc.*, **69**, 1047–1057.

Verstraete, J.-M., 1992: The seasonal upwellings in the Gulf of Guinea. *Prog. Oceanogr.*, **29**, 1–60.

Ward, M. N., and C. K. Folland, 1991: Prediction of seasonal rainfall in the North Nordeste of Brazil using eigenvectors of sea-surface temperature. *Int. J. Climatol.*, **11**, 711–743.

Woodruff, S. D., R. J. Slutz, R. L. Jenne, and P. M. Steurer, 1987: A Comprehensive Ocean-Atmosphere Data Set. *Bull. Amer. Meteor. Soc.*, **68**, 1239–1250.

Yoo, J.-M., and J. A. Carton, 1988: Outgoing longwave radiation derived rainfall in the tropical Atlantic, with emphasis on 1983–4. *J. Climate*, **1**, 1047–1054.

Zebiak, S., 1993: Air–sea interaction in the equatorial Atlantic region. *J. Climate*, **6**, 1567–1586.